Journal of Food Composition and Analysis 153 (2026) 109169

Contents lists available at ScienceDirect

Journal of Food Composition and Analysis

journal homepage: www.elsevier.com/locate/jfca

Determination of hydride-generated selenium in aqueous matrices by modified atomic fluorescence spectrometry☆

Arjun Muthu [a,b,*,1], Duyen H.H. Nguyen [a,c,f], Chaima Neji [d], Aya Ferroudj [c,e], József Prokisch [c], Hassan El-Ramady [g], Áron Béni [b]

[a] Doctoral School of Food Sciences, Faculty of Agricultural and Food Sciences and Environmental Management, University of Debrecen, 138 Böszörményi Street, Debrecen 4032, Hungary
[b] Institute of Agricultural Chemistry and Soil Science, Faculty of Agricultural and Food Sciences and Environmental Management, University of Debrecen, 138 Böszörményi Street, Debrecen 4032, Hungary
[c] Institute of Animal Science, Faculty of Agricultural and Food Sciences and Environmental Management, Biotechnology and Nature Conservation, University of Debrecen, 138 Böszörményi Street, Debrecen 4032, Hungary
[d] Institute of Nutrition, Doctoral School of Food Sciences, Faculty of Agricultural and Food Sciences and Environmental Management, University of Debrecen, 138 Böszörményi Street, Debrecen 4032, Hungary
[e] Doctoral School of Animal Husbandry, Faculty of Agriculture and Food Sciences and Environmental Management, University of Debrecen, 138 Böszörményi Street, Debrecen 4032, Hungary
[f] Institute of Life Sciences, Vietnam Academy of Science and Technology, 9/621 Vo Nguyen Giap Street, Linh Trung Ward, Thu Duc City, Ho Chi Minh 721400, Vietnam
[g] Soil and Water Department, Faculty of Agriculture, Kafrelsheikh University, Kafr El-Sheikh 33516, Egypt

ARTICLE INFO

Keywords:
Hydride generation
Selenium speciation
AFS modification
GF-AAS validation
Real sample analysis

ABSTRACT

Hydrogen selenide (H_2Se) plays a central role in selenium biochemistry, yet its quantitative determination remains analytically challenging due to its high volatility, instability, and rapid redox transformations in aqueous systems. In this study, a modified atomic fluorescence spectrometry (AFS) method was developed for the trace-level determination of hydride-derived selenium species generated as H_2Se under controlled hydride-generation conditions in aqueous systems. A low dead-volume Teflon T-junction was incorporated to improve hydride-transfer stability and gas-liquid separation efficiency. Instrumental and chemical parameters were optimized systematically. H_2Se generated from Se(IV) standards was quantitatively trapped in 0.1 mol L^{-1} NaOH and subsequently measured by AFS. This method exhibited a linear response over the range 5–1000 μg L^{-1}, with a limit of detection of 1.4 μg L^{-1}. Recovery studies in ultrapure, tap, and mineral water matrices yielded 97.3–101.8% with relative standard deviations ≤ 3.3%, indicating good accuracy and matrix tolerance. Cross-validation using graphite furnace atomic absorption spectrometry confirmed quantitative retention of selenium during the trapping step, although reduced sensitivity was observed at 5 μg L^{-1}. Overall, the proposed method provides a reproducible analytical approach for determining hydride-derived selenium species in controlled aqueous systems and in analytical studies of selenium redox transformations.

1. Introduction

Hydrogen selenide (H_2Se) is a key metabolic intermediate in selenium biochemistry, bridging inorganic selenium compounds such as selenite and selenate with biologically active forms like selenocysteine, the 21st amino acid essential for redox-regulating selenoproteins (Cupp-Sutton and Ashby, 2016; Kuganesan et al., 2019). Beyond its role as a biosynthetic precursor, H_2Se is increasingly recognized as a reactive and potentially regulatory gas transmitter with unique effects on cellular signaling, redox modulation, and enzymatic activity, which exhibits similar despite its emerging biological significance, the precise physiological behavior of H_2Se remains poorly understood, primarily due to

☆ A complete list of abbreviations is provided in the Supplementary Information

* Corresponding author at: Doctoral School of Food Sciences, Faculty of Agricultural and Food Sciences and Environmental Management, University of Debrecen, 138 Böszörményi Street, Debrecen 4032, Hungary
E-mail address: arjun.muthu@agr.unideb.hu (A. Muthu).
[1] ORCID id: 0000-0001-5297-2811

https://doi.org/10.1016/j.jfca.2026.109169
Received 30 January 2026; Received in revised form 18 March 2026; Accepted 14 April 2026
Available online 15 April 2026

substantial analytical challenges associated with its detection (Kang et al., 2022). H_2Se is extremely difficult to quantify because of its inherent chemical instability. In aqueous environments, it rapidly undergoes acid-base dissociation ($H_2Se \leftrightarrow HSe^- \leftrightarrow Se^{2-}$), autoxidation to elemental selenium (Se^0), or reaction with thiols and disulfides to form unstable selenosulfide intermediates (Hankins and Lukesh, 2024). Its gaseous nature under physiological conditions and short half-life in oxygenated media further complicates direct measurement. Endogenous H_2Se formed during the thiol-mediated reduction of selenite is transient, highly concentration-dependent, and sensitive to environmental pH and redox conditions, making real-time quantification essential for mechanistic studies (Tarze et al., 2007). However, the present study does not attempt to measure endogenous or biologically generated H_2Se; rather, it focuses on its controlled analytical generation and detection. Current speciation methods, such as gas chromatography mass spectrometry (GC-MS) (Moreno-Martin et al., 2021; Zhou et al., 2025), high-performance liquid chromatography (HPLC) (Tutar et al., 2025), and inductively coupled plasma mass spectrometry (ICP-MS) (Bierla et al., 2025; Moreno-Martín et al., 2026) are optimized for stable selenium compounds and generally require derivatization, trapping, or multi-step sample preparation. These approaches are not amenable to detecting free H_2Se in aqueous matrices, nor do they allow accurate assessment of dynamic transformations between selenium redox species (Li et al., 2025). Hydride generation atomic fluorescence spectroscopy (HG-AFS) provides an attractive alternative for selenium detection due to its high selectivity, low detection limits, and minimal matrix interference (Irizarry et al., 2001; Nakahara et al., 1980; Skok et al., 2024; Zou et al., 2018). However, standard AFS configurations are not optimized for volatile selenium hydrides. Challenges include dead volume in tubing, inefficient gas-liquid separation, and signal instability caused by turbulent flow or bubble formation (Chen and Belzile, 2010; Evans et al., 2020; Sanchez-Rodas et al., 2013). While some modifications have been proposed for detecting other hydride-forming elements (e.g., AsH_3, SbH_3)(Gao et al., 2024; Liu et al., 2025), specific adaptation for H_2Se remains underexplored (Malik et al., 2019; Sánchez-Rodas et al., 2010). To date, all reported H_2Se detection strategies rely primarily on fluorescent probes (Kong et al., 2016), which enable intracellular imaging but provide no quantitative information in environmental or aqueous matrices (Xin et al., 2020). Moreover, while reduced selenium species may form H_2Se under strongly reducing or thiol-rich conditions, no analytical method currently enables direct measurement of this transformation in aqueous media (Hu et al., 2025).

To address these challenges, the present study applies established hydride-generation design principles to minimize dead volume and improve gas–liquid transfer efficiency. A Teflon T-joint was incorporated as a low-dead-volume inline mixer, enabling controlled, laminar merging of hydrogen gas with the sample stream, thereby enhancing hydride-generation efficiency and minimizing turbulence-related signal instability. The design also reduces hydride losses associated with interactions at the tubing wall and improves transfer to the gas-liquid separator (GLS). While similar flow-path minimization approaches have been reported in hydride-generation systems for other elements, their application to the detection of hydrogen selenide in strongly alkaline matrices has received limited attention. Similar flow-path optimization strategies have been reported for hydride-forming elements such as arsenic and antimony; however, their application to selenium, particularly in the context of hydride stabilization and purge-and-trap workflows in alkaline systems, remains limited. For trapping, 0.1 mol L^{-1} NaOH was selected because its high pH (~13) promotes rapid deprotonation of dissolved H_2Se to HSe^-/Se^{2-} species, thereby reducing volatility and preventing oxidative loss during collection and storage. The use of 0.1 mol L^{-1} NaOH also minimizes the risk of re-oxidation or disproportionation of the trapped analyte, which can occur in neutral or weakly acidic conditions (Schilling and Wilcke, 2011; Ueta et al., 2020; Wickstrom et al., 1991). Previous studies on hydride generation systems have demonstrated that sodium hydroxide, at comparable molarities, provides high trapping efficiency and chemical stability for other chalcogen hydrides, including H_2S and H_2Te, due to similar dissolution and stabilization mechanisms (Cao et al., 2017; Ueta et al., 2020). Method optimization was performed using a full factorial experimental design to evaluate the effects of $NaBH_4$ concentration, NaOH composition, and gas-flow parameters on hydride formation and detection. Analytical performance was assessed by calibration, trapping efficiency, and cross-validation against GF-AAS after oxidation of the trapped species to Se(IV). In this study, H_2Se is generated in situ from Se (IV) under controlled hydride-generation conditions and used as an analytical intermediate for quantifying hydride-forming selenium species, rather than being measured as a native analyte in the original sample. The method's applicability was evaluated using ultrapure, tap, and mineral water matrices, selected as representative controlled aqueous systems. These matrices were chosen to assess hydride generation, transfer stability, and trapping efficiency under conditions relevant to analytical workflows commonly used for digested samples. The novelty of this work lies in the integration of flow-path minimization, external hydrogen-assisted hydride formation, and controlled in-line acidification into a unified HG-AFS workflow specifically adapted for unstable selenium hydrides in alkaline systems. Although the present work focuses on simplified aqueous matrices, the developed method provides a basis for future investigations involving more complex food-related systems and selenium transformation processes.

2. Materials and methods

2.1. Chemicals and reagents

Sodium selenite (Na_2SeO_3), sodium tetra borohydride ($NaBH_4$, 98%, AR grade), sodium hydroxide (NaOH), hydrochloric acid (HCl, 37%), and ammonia solution (30%) were obtained from VWR International Ltd. (Leics, UK) and Acros Organics (Belgium). Ultrapure water (18.2 MΩ cm) was produced using a Milli-Q Advantage A10 system (Merck Millipore, Germany). A 1000 mg L^{-1} selenium stock solution was prepared from Na_2SeO_3 in ultrapure water and stored in the dark. Working standards (5–1000 μg L^{-1}) were prepared daily in 0.1 mol L^{-1} NaOH to stabilize selenide/hydride-derived species during trapping and prevent volatility loss. The reductant solution (1.4% w/v $NaBH_4$ was freshly prepared in 0.1 mol L^{-1} NaOH immediately before use to prevent hydrolytic decomposition. This 1.4% (w/v) $NaBH_4$ solution was used exclusively for the initial hydride-generation step, in which Se(IV) was reduced under acidic conditions to generate H_2Se gas for trapping and the preparation of working standards. For hydride generation, 3 mol L^{-1} HCl served as the acidic reaction medium. All glassware and Teflon components were soaked in 10% HNO_3 for 12 h, rinsed extensively with ultrapure water, and verified to be free of selenium contamination by blank AFS scans prior to analysis. Although Se(IV) is known to slowly oxidize to Se(VI) in Teflon containers, freshly prepared standards were used within 2 h of preparation, minimizing oxidation-related artefacts. No measurable oxidation was detected in blank or control AFS runs.

2.2. Atomic fluorescence spectrometer configuration and instrumental modification

All fluorescence measurements were carried out using a PSA Millennium Excalibur 10.055 Atomic Fluorescence Spectrometer (PS Analytical, Orpington, UK). The system was equipped with dual-channel peristaltic pumps, a standard gas-liquid separator (GLS), quartz atomizer, photomultiplier tube detector, a drying tube, and PSA Millennium software (version 2.23). To improve the transfer stability of H_2Se, the standard manifold was modified by incorporating a low-dead-volume Teflon T-joint based on established flow-path minimization principles used in hydride-generation systems. All solutions were introduced simultaneously using synchronised peristaltic pumping to ensure consistent mixing and reproducible reaction timing within the T-joint. In

the modified design, the sample stream and 3 mol L^{-1} HCl are merged upstream for rapid in-line acidification, a controlled external H_2 gas supply is introduced, and the combined stream is immediately directed to the GLS. This externally assisted configuration provides a continuous, stable flame independent of the reductant chemistry ($NaBH_4$ & HCl) and improves signal reproducibility. The T-joint minimizes mixing volume, reduces bubble coalescence and turbulence, and shortens the hydride transport path, thereby reducing H_2Se decomposition prior to atomization. Because the sample matrix (NaOH + $NaBH_4$) is acidified in-line with 3 mol L^{-1} HCl, the resulting reaction forms only NaCl, which remains far below its solubility limit. No precipitation, clogging, or tubing deposition was observed across all experimental runs, confirming the chemical compatibility of the modified manifold. All optical and electronic parameters (lamp current, slit width, EHT voltage) were adjusted according to the manufacturer's recommended settings.

2.3. Method optimization

Method optimization was performed in two sequential stages to ensure stable hydride formation, efficient H_2Se transport, and reproducible AFS signal output. The optimization followed the workflow illustrated in Fig. 1. Method optimization was conducted in two sequential stages to improve clarity and reproducibility: (i) instrumental optimization of gas and liquid flow conditions in the modified HG-AFS manifold, and (ii) optimization of the $NaBH_4$–NaOH reagent matrix used during AFS measurement. This sequential design enabled the establishment of stable flame conditions before evaluating the influence of reagent composition on signal intensity and hydride-transfer behavior.

(a) Instrumental optimization: gas-liquid flow stability

In the first stage, a 2^2 full factorial design was applied to evaluate hydrogen gas flow rate and reagent flow rate as instrumental factors affecting flame stability and hydride transport. Only conditions producing a stable and uninterrupted flame were carried forward to the second stage. Two instrumental factors were evaluated as:

- Hydrogen gas flowrate: 0.5×10^{-6} and 1.0×10^{-6} L min^{-1}
- Reagent flow rate: 0.5 and 1.0 mL min^{-1}

These parameters directly influence the continuity of the hydride flame, mixing efficiency at the T-joint, and the transfer of volatile H_2Se to the GLS. Flame stability was assessed qualitatively (continuity, absence of flicker, atomizer noise), while peak height and integrated peak area (mAU) were recorded as quantitative responses. Only conditions producing a stable, uninterrupted flame were carried forward to chemical optimization.

(b) Reagent matrix optimization

In the second stage, a three-level factorial design was used to assess the relative composition of $NaBH_4$ and NaOH in the reagent matrix. Peak height and integrated peak area were recorded as quantitative responses, while flame continuity and atomizer noise were monitored qualitatively to support practical selection of the final operating condition. To optimize the chemical composition that promotes maximum H_2Se generation while preventing excessive foaming or turbulence. Two reagent factors were examined:

- $NaBH_4$: 10%, 40%, 70% (coded as –1, 0, +1)
- NaOH: 2%, 8%, 14%

These reagents jointly regulate reduction kinetics, solution pH, and hydride-forming efficiency inside the in-line acidification zone. Peak height and integrated peak area (mAU) were used as quantitative responses. Factor significance, interaction effects, and optimal conditions were determined through ANOVA-based model evaluation (R^2, adjusted R^2, lack of fit). A workflow diagram summarizing the optimization strategy is presented in Fig. 1. The factorial design was employed as a systematic optimization tool; however, the primary objective of the study is the development and validation of a modified HG-AFS configuration for improved hydride handling.

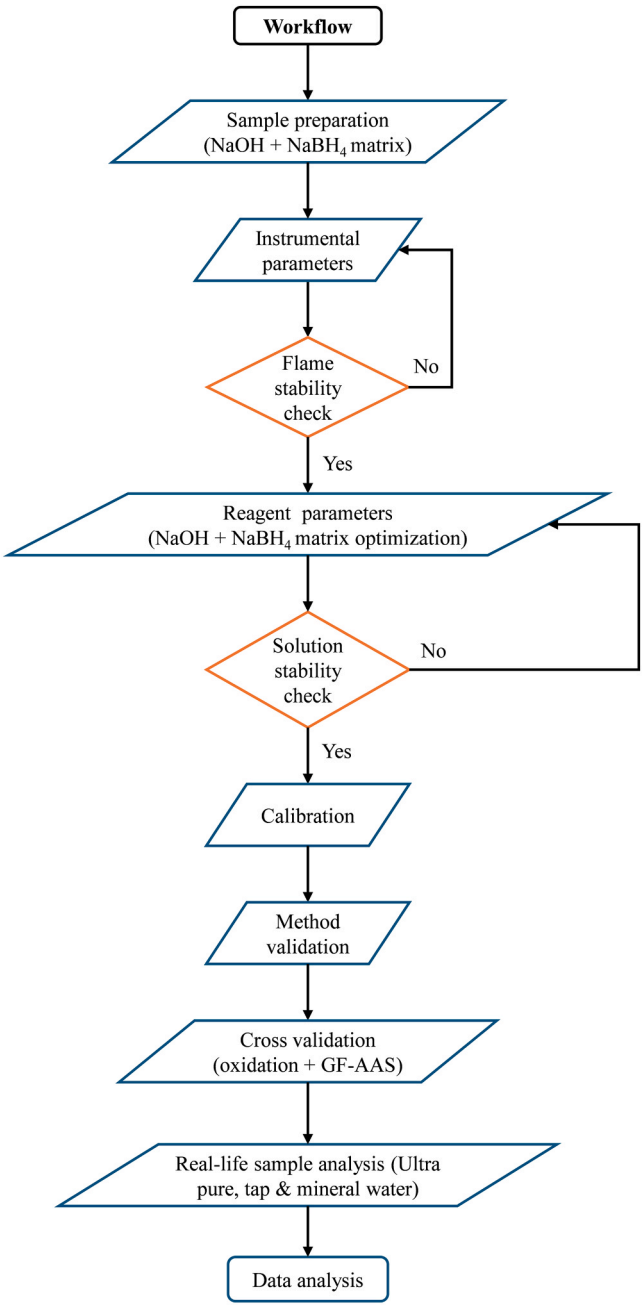

Fig. 1. Workflow diagram for the development and validation of the optimized Atomic Fluorescence Spectroscopy (AFS) method.

2.4. Method validation

Calibration was performed using seven selenium standards (5, 10, 50, 100, 250, 500, and 1000 μg L^{-1}), each prepared freshly by diluting the Se(IV) stock solution into the optimized reagent matrix. For each calibration level, the standard was mixed with the optimized NaOH-$NaBH_4$ solution immediately before analysis to ensure consistent

hydride generation conditions across all measurements. All standards were introduced into the AFS under the optimized instrumental settings, and each concentration was analyzed in triplicate. A calibration curve was constructed by plotting fluorescence intensity (mAU) against selenium concentration (μg L^{-1}), and linear regression analysis was performed. The limit of detection (LOD) and limit of quantification (LOQ) were calculated according to AOAC (AOAC International, 2016) and ICH Q2(R1) (ICH, 1995) guidelines using Eqs. (1) and (2):

$$LOD = \frac{3.3\sigma}{S} \quad (1)$$

$$LOQ = \frac{10\sigma}{S} \quad (2)$$

where σ represents the standard deviation of ten blanks (0.1 mol L^{-1} NaOH + $NaBH_4$) measured under identical conditions, and S is the slope of the calibration curve. This approach ensures that both LOD and LOQ reflect the actual background variability of the optimized hydride-generation matrix.

2.5. Trapping and recovery of H_2Se in different aqueous matrices

Method applicability and matrix tolerance were evaluated in three aqueous matrices: ultrapure water, laboratory tap water, and commercial mineral water (ALDI, Debrecen, Hungary). Aqueous systems were selected because the formation of H_2Se occurs exclusively during liquid-phase hydride reactions, and quantitative determination requires immediate stabilization of the gas in alkaline media to prevent volatilization, oxidation, or disproportionation. H_2Se was generated by reacting Se(IV) standards (5, 10, 100 μg L^{-1}) with 1.4% $NaBH_4$ and 3 mol L^{-1} HCl in a sealed hydride-generation vessel (Ueta et al., 2020). The evolved H_2Se was purged using argon (1.5×10^{-6} L min^{-1}) for 10 min and trapped in 0.1 mol L^{-1} NaOH. The NaOH absorbent for each matrix was prepared using the same water type (ultrapure, tap, or mineral) to preserve ionic composition and ensure matrix-matched trapping efficiency. Trapped hydride species were quantified by AFS. Recoveries and relative standard deviations (RSD%) were calculated from triplicate measurements to assess accuracy and matrix tolerance. The inclusion of tap and mineral water enabled assessment of potential interferences arising from naturally occurring ions (e.g., Ca^{2+}, Mg^{2+}, HCO_3^-, and Cl^-), which may affect hydride formation, purging efficiency, or trapping kinetics. The trapped H_2Se, stabilized in 0.1 mol L^{-1} NaOH, was subsequently used as the working solution for analytical measurements in the AFS system. It should be noted that H_2Se is not present in the initial samples but is generated during the hydride-generation reaction from Se (IV), and subsequently trapped and quantified. The trapping efficiency was evaluated under the selected purge conditions; however, the breakthrough capacity of the NaOH solution was not explicitly determined. Although not quantitatively determined, the trapping capacity was considered sufficient for the concentration range studied based on complete recovery and absence of signal loss during extended purging. Given the low analyte concentrations and the strong alkaline conditions that promote rapid conversion of H_2Se to non-volatile species, the trapping system was considered sufficient for the experimental range applied.

2.6. Cross-validation via graphite furnace atomic absorption spectrometry (GF-AAS)

Graphite Furnace Atomic Absorption Spectrometry (GF-AAS) was used as an independent validation tool to verify the total amount of selenium retained in the alkaline trap following hydride generation. Because GF-AAS cannot directly detect volatile H_2Se, the trapped hydride species (present predominantly as HSe^-/Se^{2-} in 0.1 mol L^{-1} NaOH) were oxidized to Se(IV), the oxidation state compatible with furnace atomization. For oxidation, each trapped solution was acidified to 2% (v/v) with concentrated HNO_3 (69%), a protocol widely used for the quantitative conversion of reduced selenium species prior to GF-AAS analysis. Oxidation ensured full dissolution, prevented volatilization, and provided a chemically uniform analyte for calibration and measurement. Analyses were performed using a Shimadzu AA-7000 GF-AAS equipped with an autosampler, deuterium background correction, and a 1% (w/v) nickel nitrate matrix modifier to improve analyte thermal stability during pyrolysis. After trapping, the same solutions were used as Calibration standards (1–150 μg L^{-1}) with 0.1 M NaOH. HNO_3 was added to oxidize, and then the matrix modifier was added. A 10 μL aliquot was injected for all measurements. The complete furnace temperature program, including drying, pyrolysis, atomization, and cleaning cycles, is provided in the Supplementary Information, Table S1. Since GF-AAS quantifies only the oxidized selenium content and does not directly detect H_2Se, its role in this study was limited to confirming the quantitative retention and recovery of selenium following purge-and-trap. Comparisons with AFS thus reflect the accuracy of the trapping process rather than the hydride-generation behavior within the furnace system.

2.7. Statistical analysis

All statistical analyses were conducted using Python 3.13 and IBM SPSS Statistics 26. Data are reported as mean ± standard deviation (SD) based on triplicate measurements (n = 3). Factorial optimization data were analysed using ANOVA to identify significant main effects and interactions. Model adequacy was assessed using F-tests, p-values, R^2, adjusted R^2, predicted R^2, and lack-of-fit statistics. The statistical analysis was applied primarily to support experimental optimization and confirm factor significance rather than to develop predictive statistical models of analytical performance. For comparison of recovery values across matrices and concentrations, Tukey's HSD test (α = 0.01) was applied. Duncan's multiple-range test was used to assign groups homogeneously where needed. All contour and surface plots were generated using Jupyter Notebook (with Matplotlib and seaborn) and Microsoft Excel.

3. Results and discussion

3.1. Instrumental optimization for hydride generation and AFS stability

In conventional HG-AFS systems, hydride generation and flame support are typically coupled through the $NaBH_4$–HCl reaction, which can lead to unstable gas evolution, particularly in alkaline matrices (Souza et al., 2022). In contrast, the present configuration decouples flame stability from reductant chemistry by introducing an external hydrogen source, allowing controlled hydride formation following in-line acidification. This modification, combined with reduced dead volume and improved mixing geometry, enhances hydride-transfer efficiency and signal reproducibility for volatile selenium species. The first stage of method development focused on improving hydride-transfer efficiency and stabilizing atomization in the modified AFS system. In the standard method, H_2 is normally produced in situ from the $NaBH_4$-HCl reaction and serves simultaneously as the reductant for hydride formation and the fuel gas for sustaining the quartz atomizer flame. However, the present workflow required selenium samples to be introduced into a strongly alkaline NaOH-$NaBH_4$ matrix, in which the conventional hydride-generation method is incompatible due to immediate hydrolysis, vigorous foaming, and unstable gas evolution. To overcome these limitations, an externally supplied hydrogen line was incorporated into the manifold to sustain the AFS flame and promote the controlled reduction of selenium species to H_2Se following in-line acidification of the alkaline sample. A low dead volume Teflon T-joint was positioned between the sample outlet and the gas-liquid separator (GLS) to ensure rapid mixing and minimize hydride decomposition before separation.

In the modified configuration (Fig. 2), the sample solution prepared in 0.1 mol L^{-1} NaOH and $NaBH_4$ is introduced through one channel (dark maroon-colored line), while a blank solution (0.1 mol L^{-1} NaOH) is used for baseline correction (green colored line). A separate stream of 3 mol L^{-1} HCl (magenta colored line) is merged with the sample immediately prior to hydride formation to ensure rapid in-line acidification. In addition, an external H_2 gas line (red line) is introduced solely to maintain a stable flame and improve atomization stability, whereas the chemical conversion of selenium species to volatile hydride still occurs via the $NaBH_4$-mediated reduction step, activated by in-line HCl acidification. Thus, the role of external H_2 is supportive rather than reductive, and hydride formation remains governed by the $NaBH_4$/HCl reaction chemistry. Immediate acidification facilitates the rapid conversion of Se(IV) to volatile H_2Se while preventing premature decomposition during transit. In the conventional method, bubble coalescence, hydride breakdown, and back-pressure formation typically occur. Relocating the mixing point to a low-volume connector positioned close to the GLS greatly reduced these losses, producing smoother flow profiles, reduced flame flicker, lower baseline noise, and improved transport of freshly formed hydride. Fig. 3(a) shows the 2D view of the AFS equipment before the modification, and (b) represents the 2D view of the equipment after the modifications.

To identify optimal operational parameters, a two-factor full factorial design was applied, evaluating hydrogen flow rate (0.5×10^{-6} and 1.0×10^{-6} L min^{-1}) and reagent flow rate (0.5 and 1.0 mL min^{-1}). Only the high-flow combination (Run E2) produced a stable flame, consistent hydride introduction, and reproducible signals. All other combinations resulted in intermittent atomization, insufficient hydride formation, or turbulence-driven loss of precision (Supplementary Information tables S2 and S3). Overall, this externally assisted hydride-generation strategy addresses the key limitations noted in previous hydride-generation configurations, namely dead-volume-induced turbulence, insufficient reduction in alkaline matrices, and hydride decomposition during transport. The optimized configuration improves hydride-transfer stability and signal reproducibility for trace-level detection of selenium via hydride-derived species generated as H_2Se in the modified HG-AFS workflow. Similar flame optimization strategies have been reported in hydride generation systems for arsenic and antimony detection (Rahman et al., 2000; Wietecha-Posłuszny et al., 2006), though their application to selenium, particularly in volatile hydride form, remains limited (Murillo et al., 2008). The current setup thus provides a tailored solution for trace H_2Se detection while maintaining AFS signal stability and operational simplicity.

3.2. Optimization of reagent composition

The optimization results are interpreted in the context of improving hydride-generation stability and transfer efficiency within the modified manifold, rather than as an independent chemometric study. Following instrumental optimization, the chemical composition of the reagent system used during AFS measurement was evaluated to maximize signal response and hydride stability. It is important to note that this optimization does not refer to the initial hydride-generation step used in standard preparation, in which H_2Se is generated from Se(IV) using 1.4% (w/v) $NaBH_4$ under acidic conditions. Instead, the optimization focuses on the reagent environment within the AFS system during measurement. Although the modified AFS manifold employs externally supplied hydrogen to stabilize the atomizer flame and assist in-line reduction, the primary formation of H_2Se occurs inside the sealed hydride-generation reactor, where Se(IV) reacts with $NaBH_4$ under alkaline conditions. The efficiency of H_2Se generation depends critically on the concentration of both the reducing agent ($NaBH_4$) and the alkali stabilizer (NaOH), which control reaction kinetics, pH, and stability of the intermediate species (Bax et al., 1986; Elsayed et al., 2000). Supplementary Information table S4 presents the parameters for reagent optimization and the levels selected for optimization. A two-factor, three-level full factorial design was employed to investigate the effects of $NaBH_4$ (10%, 40%, 70%) and NaOH (2%, 8%, 14%) on the fluorescence signal intensity (mAU). The $NaBH_4$ (10%, 40%, 70%) values represent the relative composition of the $NaBH_4$–NaOH reagent system used during AFS analysis. The experimental matrix and corresponding responses are shown in Table 1. The highest observed signal intensity (6300.49 mAU) was recorded at 70% $NaBH_4$ and 14% NaOH. However, this condition was not selected as the final working condition because higher reagent levels led to excessive gas evolution and less stable hydride-transfer behavior. In contrast, 40% $NaBH_4$ and 8% NaOH provided a more favorable balance among signal intensity, reductive efficiency, and operational stability. Therefore, it was selected as the practical operating condition for subsequent calibration and sample analysis. At higher $NaBH_4$ levels (70%), excessive hydrogen evolution occurred, leading to vigorous foaming and gas–liquid disturbance that impaired consistent hydride transfer to the atomizer (Wang and Tyson, 2014). Conversely, at lower $NaBH_4$ concentrations (10%), reductant availability was insufficient for complete conversion of Se(IV) to volatile H_2Se (Suzuki et al., 2012). The contour and surface plots (Figs. 4 & 5) clearly illustrate the strong positive influence of $NaBH_4$ concentration on signal intensity.

Statistical analysis using ANOVA revealed that $NaBH_4$ concentration had a significant influence on signal intensity ($p = 0.013$) (Supplementary Information table S5), whereas the effect of NaOH concentration and the interaction term were not statistically significant ($p > 0.05$). Although NaOH had a smaller effect on signal magnitude, its role in stabilizing $NaBH_4$, controlling the reaction pH, and preventing premature decomposition of intermediate hydride species remains critical. The model showed a good fit with an R^2 of 81.8% and a standard error of 1322.21 (Table 2). These results support the selection of 40%

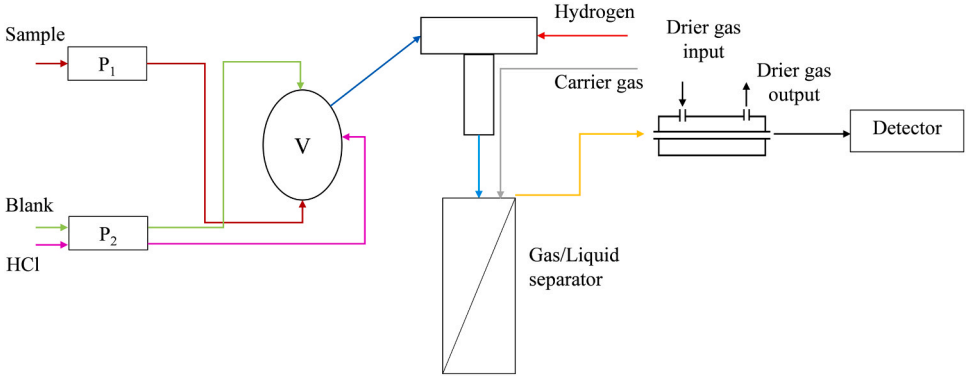

Fig. 2. Modified flow injection system for Hydrogen selenide (H_2Se) detection. P_1 and P_2: Peristaltic pumps; V: Valve system; Gas-liquid separator and drier modules are integrated before signal detection.

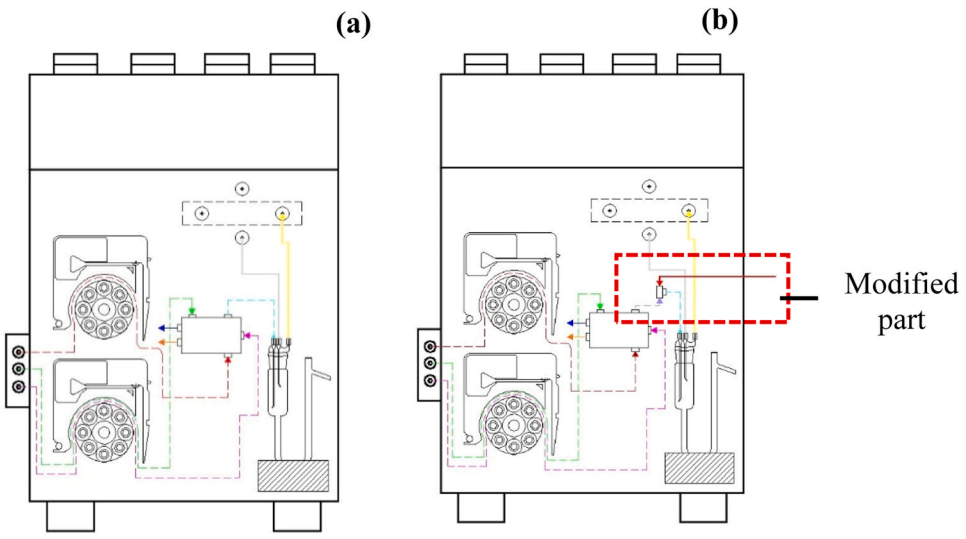

Fig. 3. (a) 2D representation of the Atomic Fluorescence Spectroscopy (AFS) Instrument before modification and (b) after modification. Colored pathways indicate separate fluid and gas lines.

Table 1
Reagent experimental design matrix.

Runs	$NaBH_4$ (%)	NaOH (%)	Response (signal, mAU)
E_1	0	0	5220.00
E_2	1	-1	6000.22
E_3	0	0	5220.43
E_4	1	1	6300.49
E_5	0	0	5210.35
E_6	-1	-1	500.49
E_7	0	0	5230.31
E_8	-1	1	600.43

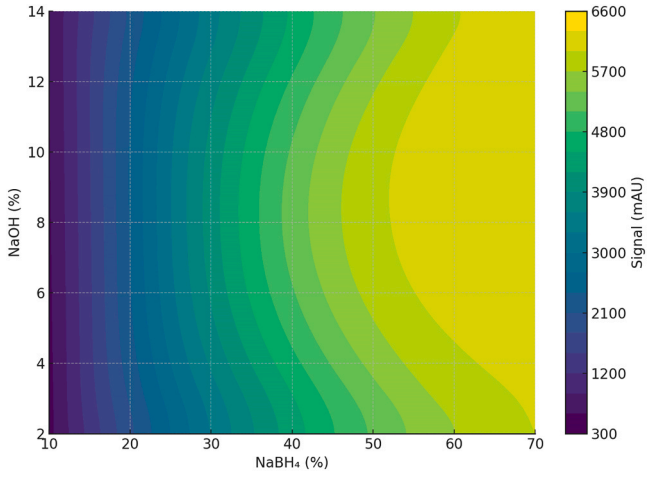

Fig. 4. Contour plot showing the influence of Sodium borohydride ($NaBH_4$) and sodium hydroxide (NaOH) concentrations on signal intensity (mAU).

$NaBH_4$ in 8% NaOH as the practical operating condition for subsequent measurements, considering both signal response and system stability. These findings are consistent with previous works, that moderate $NaBH_4$ concentrations enhanced signal strength in hydride generation AFS for arsenic detection, while excessive reductant led to reduced precision (Abdel-Lateef et al., 2013; Shraim et al., 1999). However, few studies have optimized this matrix specifically for H_2Se, underlining the novelty of the present approach in establishing conditions that maximize both signal intensity and stability for this volatile analyte (Kratzer and

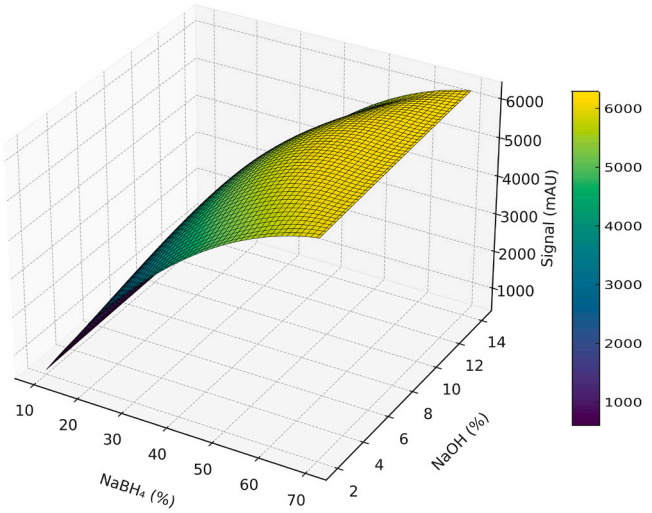

Fig. 5. 3D surface plot representing the signal response (mAU) as a function of Sodium borohydride ($NaBH_4$) and sodium hydroxide (NaOH) concentrations.

Table 2
Model summary.

S	R^2	R^2- (adj)	R^2-(pred)
1322.21	81.79%	68.13%	0.00%

Dědina, 2007).

3.3. Method validation

The analytical signal obtained in this study corresponds to hydride-derived selenium generated during the reduction of Se(IV), rather than direct measurement of pre-existing H_2Se in the sample matrix.

3.3.1. Limit of detection (LOD) and limit of quantification (LOQ)

The quantitative performance of the optimized method was evaluated by constructing a seven-point calibration curve using selenium standards at concentrations of 5, 10, 50, 100, 250, 500, and 1000 μg L^{-1}. Fluorescence intensity was plotted against concentration,

and the curve showed excellent linearity across the tested range, with a regression coefficient of determination $R^2 = 0.9973$, indicating a strong correlation between signal and analyte concentration (Fig. 6). The regression equation was derived as:

$$Signal(mAU) = 1.599 \times [Se] - 14.91$$

where [Se] is the selenium concentration in μg L^{-1}. The regression slope was statistically significant ($p < 0.0001$).

The limit of detection (LOD) is 1.4 μg L^{-1}, and the limit of quantification (LOQ) is 4.2 μg L^{-1}, which were calculated according to AOAC (AOAC International, 2016) and ICH Q2(R1) (ICH, 1995) guidelines using the standard deviation of the blank (σ) and the slope (S) of the calibration curve, as described in the Section 2.4. These values demonstrate that the method is sufficiently sensitive to detect trace levels of selenium in environmental and aqueous matrices, particularly as selenium via hydride-derived species generated as H_2Se under controlled conditions. Compared to conventional approaches, the modified AFS system exhibits strong analytical performance. Previous studies utilizing hydride generation with atomic absorption spectroscopy (HG-AAS) or ICP-MS reported comparable or slightly lower LODs; however, these methods often require more complex instrumentation, pre-reduction steps, or inert gas shielding to stabilize reactive selenium intermediates (Haygarth et al., 1993; Li et al., 2012). The current method achieves comparable sensitivity with a simplified setup and minimal sample handling, offering a more accessible and cost-effective solution for selenium speciation. Repeatability across calibration levels was consistently < 5% RSD, and signal stability was maintained over multiple runs, confirming the robustness of the modified system. Conventional HG-AFS methods typically achieve detection limits in the ng L^{-1} range under direct measurement conditions (Nakahara et al., 1980; Sanchez-Rodas et al., 2013). In contrast, the higher LOD observed in this study (1.4 μg L^{-1}) results from a multi-step workflow that includes hydride generation, purge-and-trap collection, and subsequent analysis of the trapped solution. These steps introduce dilution and increased background variability associated with the alkaline trapping medium. Similar increases in detection limits have been reported in purge-and-trap-based hydride systems and multi-step analytical workflows (Ueta et al., 2020). Therefore, the present method prioritizes controlled hydride stabilization and reproducibility over the achievement of ultra-trace detection limits. It is important to note that the developed HG-AFS workflow does not provide comprehensive speciation of selenium in complex food or biological matrices. Instead, the method quantifies hydride-derived selenium species generated as hydrogen selenide under controlled hydride-generation conditions. Consequently, the analytical performance demonstrated here reflects the method's sensitivity in detecting reduced selenium species that can form volatile hydrides (Sanchez-Rodas et al., 2013). While this capability may support mechanistic studies of selenium redox transformations or analytical workflows involving hydride-generation reactions, additional separation techniques, such as chromatographic speciation methods, would be required to complete the characterization of multiple selenium species in complex biological or food-derived samples (Ferreira et al., 2022).

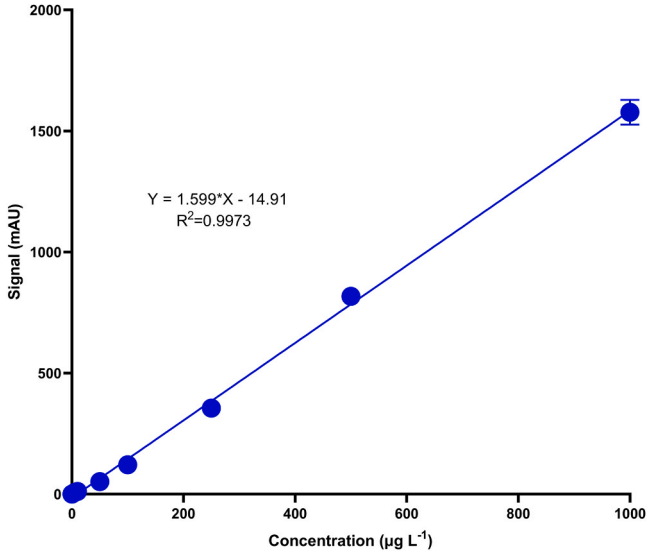

Fig. 6. Calibration curve of selenium standards (5–1000 μg L^{-1}) measured using the optimized Atomic Fluorescence Spectroscopy (AFS) method.

3.3.2. *Recovery and spiking of H_2Se*

The accuracy and trapping efficiency of the developed AFS method were evaluated using spike and recovery experiments performed at two concentration levels (5 and 100 μg L^{-1}) across three aqueous matrices: ultrapure water, tap water, and commercial mineral water. All samples were prepared in the optimized NaOH-$NaBH_4$ matrix; the spiking experiments also evaluated the stability of hydride formation. In each case, Se(IV) standards were reduced with 1.4% $NaBH_4$ in the presence of 3 mol L^{-1} HCl under the optimized hydride-generation conditions, generating volatile H_2Se. The evolved gas was carried by argon into 0.1 mol L^{-1} NaOH, prepared using the corresponding matrix. The trapped selenium species were quantified using the modified AFS system. Fig. S1 (Supplementary Information Section) shows the schematic representation of the spiking experiment. Table 3 shows the recovery efficiency of the AFS method with various aqueous matrices with different spiked concentrations. Across all matrices and spike levels, recoveries ranged from 97.31% to 101.77%, with RSD values below 3.3% (Table 3). Recoveries slightly exceeding 100% may be attributed to localized pH enhancement effects, improved bubble stabilization in the GLS, or minor spectral overlap, phenomena previously observed in hydride-based systems (Greda et al., 2015; Lampugnani et al., 2003). The consistency of recoveries across the tap and mineral water indicates that dissolved ions typically present in drinking water (e.g., Ca^{2+}, Mg^{2+}, HCO_3^-, Cl^-) do not significantly influence hydride formation or H_2Se capture. These results align with previous findings that variable recovery of volatile selenium species depends on reductant concentration, reaction time, and carrier gas flow (Chatterjee et al., 2001; Suzuki et al., 2012). Importantly, no statistically significant differences were observed between matrices or spike levels (Tukey's HSD, $p > 0.05$), demonstrating the robustness of the method in diverse aqueous conditions. These findings demonstrate that the developed AFS approach reliably quantifies hydride-derived selenium species under controlled analytical conditions and may support future investigations of selenium redox transformations in aqueous systems. Comparable recoveries (94–102%) have been reported for selenium in drinking water using hydride-generation ICP-MS, although those workflows required extensive pretreatment and inert gas shielding (Robberecht and Van Grieken, 1982).

It should be noted that the present validation was conducted

Table 3
Recovery efficiency and precision of Hydrogen Selenide (H_2Se) detection in real samples.

Sample	Spiked concentration (μg L^{-1})	Recovery (%)	RSD (%)
Ultra-pure water	100	101.77 ± 0.9[a]	0.82
	5	99.76 ± 1.6[a]	2.48
Tap water	100	99.77 ± 1.70[a]	1.71
	5	97.31 ± 2.10[a]	2.15
Mineral water	100	100.43 ± 0.91[a]	0.90
	5	101.01 ± 2.81[a]	3.26

Data are presented as mean ± SD (n = 3). Superscript letters indicate statistically nonsignificant differences between groups based on Tukey's HSD test (p >0.05).

primarily using spike-and-recovery experiments in relatively simple aqueous matrices, which confirm the efficiency of hydride generation, trapping, and detection under controlled analytical conditions. However, the method's applicability to complex matrices requires further investigation, as components such as dissolved organic matter, proteins, lipids, thiol-containing compounds, and sulfide species may influence the kinetics of hydride formation and trapping efficiency. In typical analytical workflows, food samples are subjected to acid digestion (e.g., HNO_3/H_2O_2), converting selenium species into soluble inorganic forms, predominantly Se(IV) and Se(VI), which are amenable to hydride generation. Under such conditions, the proposed method could be extended to quantify hydride-forming selenium fractions, although additional clean-up or masking strategies may be necessary to minimize matrix effects. Furthermore, the breakthrough volume and maximum trapping capacity of the NaOH solution were not systematically evaluated and should be addressed in future studies. Therefore, further work is required to validate the method in complex food and biological matrices and to assess matrix-specific interferences under realistic analytical conditions.

3.3.3. *Cross-validation using graphite furnace atomic absorption spectrometry (GF-AAS)*

GF-AAS was used to confirm the total amount of selenium recovered in the NaOH trap after hydride generation, as GF-AAS is a well-established reference technique for trace elemental analysis. Trapped H_2Se is present as HSe^-/Se^{2-}, all solutions were oxidized to Se(IV) prior to GF-AAS detection. This oxidation step converts all trapped hydride species into the same oxidation state, ensuring matrix-matched quantification during furnace atomization. GF-AAS to serve as a validation tool, rather than a direct detector of volatile hydrides. As shown in Table 4, recovery values of 60.2 ± 0.34% for 5 μg L^{-1} and 100.9 ± 0.30% for 100 μg L^{-1} were obtained, with RSDs of 0.24% and 3.26%, respectively. The quantitative recovery at 100 μg L^{-1} agrees closely with the AFS results, confirming the efficiency of the purge-and-trap process at moderate concentrations. In contrast, the lower recovery observed at 5 μg L^{-1} requires careful interpretation. While GF-AAS is widely used for trace selenium determination, its analytical performance (Kratzer and Dědina, 2007), can decline at low concentrations due to background noise, atomization inefficiencies, and matrix effects. In addition, because the trapped hydride species must first be oxidized to Se(IV) prior to GF-AAS analysis, the possibility of minor losses during trapping or oxidation cannot be completely excluded at very low concentrations. Similar concentration-dependent losses have been documented in hydride-related selenium studies, particularly when operating near the method's sensitivity threshold (Ding and Sturgeon, 1996; Kratzer and Dědina, 2007). Therefore, the GF-AAS comparison should be interpreted primarily as supportive confirmation of selenium retention in the trapping solution, rather than as definitive evidence of efficient trapping at the lowest concentration. In contrast, the modified AFS method directly detects hydride-derived selenium species and provides consistent recoveries across all spike levels in the tested aqueous matrices. This is attributed to higher susceptibility to background noise and incomplete atomization at low concentrations.

Tukey's HSD test indicated significant differences between spike levels ($p < 0.001$), with 100 μg L^{-1} assigned to Group A and 5 μg L^{-1} to Group B, demonstrating that GF-AAS performance declines at ultra-trace concentrations. In contrast, the modified AFS method provided consistent recoveries across all spike levels and matrices, confirming its improved sensitivity under the tested conditions for volatile selenium determination. Unlike GF-AAS, which detects selenium only after oxidation and high-temperature atomization, AFS responds directly to hydride-derived species, enabling improved detection limits, reduced sample handling, and greater analytical stability. These advantages position the modified AFS workflow as a more reliable and operationally efficient platform for trace-level H_2Se analysis, particularly in aqueous matrices where hydride behavior plays a critical role (Heilier et al., 2005).

Table 4
Recovery efficiency and precision of selenium detection using Graphite Furnace Atomic Absorption Spectroscopy (GF-AAS).

Sample (μg L^{-1})	Recovery (%)	RSD (%)
5	60.2 ± 0.34[b]	0.24
100	100.9 ± 0.30[a]	3.26

Data are presented as mean ± SD (n = 3). Superscript letters indicate statistically significant differences between groups based on Tukey's HSD test ($p < 0.001$).

The developed AFS method demonstrated acceptable analytical accuracy within the tested aqueous matrices while employing a relatively simple workflow. These results support its usefulness for controlled hydride-generation studies and suggest potential for broader application following further validation. Table 5 compares this study with previously reported methods, along with their LODs and applications.

Methods based on fluorescent probes, such as ESIPT-based ratio metric sensors (Xin et al., 2020), Hcy-H_2Se conjugates (Kong et al., 2017), near-infrared fluorophores (Kong et al., 2016), and activatable probes (Tian et al., 2019) are primarily applied in biological contexts, especially for cell imaging (e.g., HepG2 cells), and offer high specificity but are generally not optimized for selenium transformation studies or aqueous matrices. In comparison, conventional HG-AFS-based methods, such as D-CPE–HG-AFS (Wang et al., 2017) and MSFIA–HG-AFS (Souza et al., 2022), achieve significantly lower detection limits due to direct hydride generation and immediate atomization without intermediate trapping steps. However, these methods are primarily designed to determine stable selenium species (e.g., Se(IV) or total selenium) in complex matrices such as food and beverages. In contrast, the modified AFS method developed in this study focuses on the controlled generation, trapping, and quantification of hydride-derived selenium species formed as H_2Se. The inclusion of a purge-and-trap step enables stabilization of this highly volatile and reactive intermediate, albeit with a low limit of detection (1.40 μg L^{-1}) over a broad linear range (5–1000 μg L^{-1}) and consistent analytical performance across aqueous

Table 5
Comparison of reported analytical methods for hydrogen selenide (H_2Se) detection, including detection limits, linear ranges, and application matrices.

Method	Target species	LOD (μg L^{-1})	Linear range (μg L^{-1})	Sample matrix used	Ref.
ESIPT-based ratiometric fluorescent probe	H_2Se	16.2	0–7288	-	(Xin et al., 2020)
Fluorescent probe (Hcy-H_2Se)	H_2Se	55.1	0–8098	Cell imaging (HepG2 cells)	(Kong et al., 2017)
Near-infrared fluorescent	H_2Se	0.57	0–972	Cell imaging (HepG2 cells)	(Kong et al., 2016)
Activatable fluorescent probe	H_2Se	92.7	0–1215	Cell imaging (HepG2 cells)	(Tian et al., 2019)
D-CPE method with HG-AFS	Total Se	0.023	0.5–6.0	Food samples	(Wang et al., 2017)
MSFIA-HG-AFS	Total inorganic Se, Se (IV)	0.02 0.02	0.08–5.0 0.07–5.0	Beer samples	(Souza et al., 2022)
Modified AFS	Hydride-derived H_2Se	1.40	0–1000	water	This study

matrices, demonstrating its suitability for trace-level quantification under controlled conditions. Overall, the developed approach complements existing AFS-based techniques by enabling the study of hydride formation and transformation processes and by providing a methodological basis for future extensions to more complex systems, including digested food matrices.

4. Future perspectives and limitations

The developed AFS method provides sensitive and reliable determination of hydride-derived selenium species generated as H_2Se in controlled aqueous matrices; however, its applicability to complex food digests, biological fluids, or high-salinity samples has not yet been evaluated and will require further validation. Future studies should focus on extending the method to more complex food-related matrices and assessing the influence of dissolved organic matter, sulfide or thiol-containing compounds on hydride generation and trapping efficiency. Further studies are required to develop appropriate sample pretreatment strategies, such as digestion, dilution, or chemical masking, prior to hydride generation. Coupling the present method with chromatographic separation techniques may also be necessary for comprehensive selenium speciation in complex systems. In addition, investigations into the stability of trapped reduced selenium species during storage and handling would further strengthen the method's applicability. These developments will be essential for broadening the use of the method in food-related analytical systems, environmental water matrices and selenium transformation studies.

5. Conclusion

This study presents an integrated and experimentally validated workflow for quantifying hydride-derived selenium species generated as hydrogen selenide (H_2Se) in controlled aqueous matrices using a modified atomic fluorescence spectroscopy (AFS) platform. The key advancement lies in the redesigned HG-AFS configuration, which incorporates a low-dead-volume Teflon T-joint that enhances hydride transfer efficiency, reduces signal instability, and enables reliable operation under alkaline conditions. Factorial optimization identified 40% $NaBH_4$ in 8% NaOH and a hydrogen flow rate of 1.0×10^{-6} L min^{-1} as optimal conditions, providing a balance between signal intensity and system stability. The method demonstrated excellent linearity over the range of 5–1000 μg L^{-1} ($R^2 = 0.9973$), with limits of detection and quantification of 1.4 μg L^{-1} and 4.2 μg L^{-1}, respectively. Recovery experiments across ultrapure, tap, and mineral water matrices yielded values of 97.31–101.77% with RSDs below 3.3%, confirming high accuracy and minimal matrix interference in aqueous systems. Cross-validation using GF-AAS further verified the quantitative efficiency of the trapping step and highlighted the robustness of the developed approach. While the current work is limited to controlled aqueous matrices, the method provides a practical foundation for investigating selenium transformations and for future extension to more complex matrices, including food and biological systems, following appropriate sample preparation.

CRediT authorship contribution statement

Arjun Muthu: Writing – original draft, Visualization, Software, Methodology, Investigation, Formal analysis, Data curation, Conceptualization. **Hassan El-Ramady:** Writing – review & editing. **Áron Béni:** Validation, Supervision, Resources, Project administration, Funding acquisition. **Aya Ferroudj:** Methodology. **József Prokisch:** Validation, Resources, Funding acquisition, Conceptualization. **Duyen H.H. Nguyen:** Validation, Methodology. **Chaima Neji:** Software, Methodology.

Declaration of Competing Interest

The authors declare that they have no known competing financial interests or personal relationships that could have appeared to influence the work reported in this paper.

Acknowledgments

The authors would like to thank the Stipendium Hungaricum Scholarship program and the University of Debrecen Scientific Research Bridging Fund (DETKA). The University of Debrecen Program for Scientific Publication supports the article.

Appendix A. Supporting information

Supplementary data associated with this article can be found in the online version at doi:10.1016/j.jfca.2026.109169.

Data availability

Data will be made available on request.

References

Abdel-Lateef, A.M., Mohamed, R.A., Mahmoud, H.H., 2013. Determination of arsenic (III) and (V) species in some environmental samples by atomic absorption spectrometry. Adv. Chem. Sci. 2, 110–113.

AOAC International, 2016. Official Methods of Analysis of AOAC International. Benjamin Franklin Station, Washington DC.

Bax, D., Peters, F.F., Van Noort, J.P.M., Agterdenbos, J., 1986. The determination of selenium with hydride generation AAS—II: The role of sodium borohydride and of hydrogen gas. Spectrochim. Acta Part B At. Spectrosc. 41, 275–282. https://doi.org/10.1016/0584-8547(86)80168-9.

Bierla, K., Siwulski, M., Ouerdane, L., Lobinski, R., Mleczek, P., Mleczek, M., 2025. Identification of new selenium compounds produced by edible mushrooms. Food Chem. 496, 146763. https://doi.org/10.1016/j.foodchem.2025.146763.

Cao, G., Xu, F., Wang, S., Xu, K., Hou, X., Wu, P., 2017. Gold nanoparticle-based colorimetric assay for selenium detection via hydride generation. Anal. Chem. 89, 4695–4700. https://doi.org/10.1021/acs.analchem.7b00337.

Chatterjee, A., Shibata, Y., Yoneda, M., Banerjee, R., Uchida, M., Kon, H., Morita, M., 2001. Identification of volatile selenium compounds produced in the hydride generation system from organoselenium compounds. Anal. Chem. 73, 3181–3186. https://doi.org/10.1021/ac001356w.

Chen, Y.-W., Belzile, N., 2010. High performance liquid chromatography coupled to atomic fluorescence spectrometry for the speciation of the hydride and chemical vapour-forming elements As, Se, Sb and Hg: a critical review. Anal. Chim. Acta 671, 9–26. https://doi.org/10.1016/j.aca.2010.05.011.

Cupp-Sutton, K., Ashby, M., 2016. Biological chemistry of hydrogen selenide. Antioxidants 5, 42. https://doi.org/10.3390/antiox5040042.

Ding, W.-W., Sturgeon, R.E., 1996. Evaluation of electrochemical hydride generation for the determination of arsenic and selenium in sea water by graphite furnace atomic absorption with in situ concentration. Spectrochim. Acta Part B At. Spectrosc. 51, 1325–1334. https://doi.org/10.1016/0584-8547(96)01514-5.

Elsayed, M., Björn, E., Frech, W., 2000. Optimisation of operating parameters for simultaneous multi-element determination of antimony, arsenic, bismuth and selenium by hydride generation, graphite atomiser sequestration atomic absorption spectrometry. J. Anal. At. Spectrom. 15, 697–703. https://doi.org/10.1039/A908635H.

Evans, E.H., Pisonero, J., Smith, C.M., Taylor, R.N., 2020. Atomic spectrometry update: review of advances in atomic spectrometry and related techniques. J. Anal. At. Spectrom. 35, 830–851.

Ferreira, S.L.C., Cerda, V., Portugal, L.A., Gonçalves, L.B., Santos Neto, J.H., Pereira Junior, J.B., Palacio, E., 2022. State of the art of the methods proposed for selenium speciation analysis by CVG-AFS. Trends Anal. Chem. 152, 116617. https://doi.org/10.1016/j.trac.2022.116617.

Gao, Y.-Y., Yang, X.-A., Zhang, W.-B., 2024. High sensitivity atomic fluorescence spectroscopy for the detection of AsIII by selective electrolysis of arsenic on nanoflowers-like Fe/NFE. Talanta 275, 126127. https://doi.org/10.1016/j.talanta.2024.126127.

Greda, K., Jamroz, P., Jedryczko, D., Pohl, P., 2015. On the coupling of hydride generation with atmospheric pressure glow discharge in contact with the flowing liquid cathode for the determination of arsenic, antimony and selenium with optical emission spectrometry. Talanta 137, 11–17. https://doi.org/10.1016/j.talanta.2014.11.073.

Hankins, R.A., Lukesh, J.C., 2024. An Examination of chemical tools for hydrogen selenide donation and detection. Molecules 29, 3863. https://doi.org/10.3390/molecules29163863.

Haygarth, P.M., Rowland, A.P., Stürup, S., Jones, K.C., 1993. Comparison of instrumental methods for the determination of total selenium in environmental samples. Analyst 118, 1303–1308. https://doi.org/10.1039/AN9931801303.

Heilier, J.-F., Buchet, J.-P., Haufroid, V., Lison, D., 2005. Comparison of atomic absorption and fluorescence spectroscopic methods for the routine determination of urinary arsenic. Int. Arch. Occup. Environ. Health 78, 51–59. https://doi.org/10.1007/s00420-004-0562-x.

Hu, J., Liang, W., Yi, L., 2025. Strategies for the development of donors and precursors of hydrogen selenide (H2Se). Chem. Asian J. 20, e00842. https://doi.org/10.1002/asia.202500842.

ICH, 1995. Q2(R1) Validation of Analytical Procedures: Text and Methodology. European Medicines Agency.

Irizarry, R., Moore, J., Cai, Y., 2001. Atomic fluorescence determination of selenium using hydride generation technique. Int. J. Environ. Anal. Chem. 79, 97–109. https://doi.org/10.1080/03067310108035902.

Kang, X., Huang, H., Jiang, C., Cheng, L., Sang, Y., Cai, X., Dong, Y., Sun, L., Wen, X., Xi, Z., Yi, L., 2022. Cysteine-activated small-molecule H2Se donors inspired by synthetic H2S donors. J. Am. Chem. Soc. 144, 3957–3967. https://doi.org/10.1021/jacs.1c12006.

Kong, F., Ge, L., Pan, X., Xu, K., Liu, X., Tang, B., 2016. A highly selective near-infrared fluorescent probe for imaging H 2 Se in living cells and in vivo. Chem. Sci. 7, 1051–1056. https://doi.org/10.1039/C5SC03471J.

Kong, F., Zhao, Y., Liang, Z., Liu, X., Pan, X., Luan, D., Xu, K., Tang, B., 2017. Highly selective fluorescent probe for imaging H_2 Se in living cells and in vivo based on the disulfide bond. Anal. Chem. 89, 688–693. https://doi.org/10.1021/acs.analchem.6b03136.

Kratzer, J., Dědina, J., 2007. Arsine and selenium hydride trapping in a novel quartz device for atomic-absorption spectrometry. Anal. Bioanal. Chem. 388, 793–800. https://doi.org/10.1007/s00216-006-1048-3.

Kuganesan, M., Samra, K., Evans, E., Singer, M., Dyson, A., 2019. Selenium and hydrogen selenide: essential micronutrient and the fourth gasotransmitter? Intensive Care Med. Exp. 7, 71. https://doi.org/10.1186/s40635-019-0281-y.

Lampugnani, L., Salvetti, C., Tsalev, D.L., 2003. Hydride generation atomic absorption spectrometry with different flow systems and in-atomizer trapping for determination of cadmium in water and urine—overview of existing data on cadmium vapour generation and evaluation of critical parameters. Talanta 61, 683–698. https://doi.org/10.1016/S0039-9140(03)00324-2.

Li, H., Luo, Y., Li, Z., Yang, L., Wang, Q., 2012. Nanosemiconductor-based photocatalytic vapor generation systems for subsequent selenium determination and speciation with atomic fluorescence spectrometry and inductively coupled plasma mass spectrometry. Anal. Chem. 84, 2974–2981. https://doi.org/10.1021/ac3001995.

Li, Y., Wang, C., Zhao, J., Liu, X., Ma, M., Gao, A., Sun, K., 2025. A systematic review of separation/preconcentration and detection techniques for speciation analysis of arsenic and selenium in water. Anal. Methods 17, 5807–5830. https://doi.org/10.1039/D5AY00626K.

Liu, X., Yang, X., Chu, X., Zhang, W., 2025. Rapid determination of Se(IV) and *t*Se in fungal samples by foam electrode-based electrolytic hydride generation coupled atomic fluorescence spectrometry. Talanta 285, 127324. https://doi.org/10.1016/j.talanta.2024.127324.

Malik, L.A., Bashir, A., Qureashi, A., Pandith, A.H., 2019. Detection and removal of heavy metal ions: a review. Environ. Chem. Lett. 17, 1495–1521. https://doi.org/10.1007/s10311-019-00891-z.

Moreno-Martin, G., Sanz-Landaluze, J., León-González, M.E., Madrid, Y., 2021. vivo quantification of volatile organoselenium compounds released by bacteria exposed to selenium with HS-SPME-GC-MS. Effect of selenite and selenium nanoparticles. Talanta 224, 121907. https://doi.org/10.1016/j.talanta.2020.121907.

Moreno-Martín, G., Rodríguez-Marín, M., Queipo-Abad, S., Madrid, Y., 2026. Tracking the metabolism of selenium compounds in Spinacia oleracea using multiple stable isotope tracers and HPLC-(ID)-ICP-MS. Anal. Chim. Acta 1381, 344791. https://doi.org/10.1016/j.aca.2025.344791.

Murillo, M., Carrión, N., Colmenares, J., Romero, J., Alvarado, G., Ríos, M., Angulo, F., 2008. Design and evaluation of a continuous flow, integrated nebulizer-hydride generator for flame atomic absorption spectrometry. QuíM. Nova 31, 1315–1318. https://doi.org/10.1590/S0100-40422008000600008.

Nakahara, T., Kobayashi, S., Wakisaka, T., Musha, S., 1980. The determination of trace amounts of selenium by hydride generation-nondispersive flame atomic fluorescence spectrometry. Appl. Spectrosc. 34, 194–200. https://doi.org/10.1366/0003702804730619.

Rahman, L., Corns, W.T., Bryce, D.W., Stockwell, P.B., 2000. Determination of mercury, selenium, bismuth, arsenic and antimony in human hair by microwave digestion atomic fluorescence spectrometry. Talanta 52, 833–843. https://doi.org/10.1016/S0039-9140(00)00436-7.

Robberecht, H., Van Grieken, R., 1982. Selenium in environmental waters: determination, speciation and concentration levels. Talanta 29, 823–844. https://doi.org/10.1016/0039-9140(82)80252-X.

Sanchez-Rodas, D., Mellano, F., Morales, E., Giraldez, I., 2013. A simplified method for inorganic selenium and selenoaminoacids speciation based on HPLC–TR–HG–AFS. Talanta 106, 298–304. https://doi.org/10.1016/j.talanta.2012.11.005.

Sánchez-Rodas, D., Corns, W.T., Chen, B., Stockwell, P.B., 2010. Atomic fluorescence spectrometry: a suitable detection technique in speciation studies for arsenic, selenium, antimony and mercury. J. Anal. At. Spectrom. 25, 933–946. https://doi.org/10.1039/B917755H.

Schilling, K., Wilcke, W., 2011. A method to quantitatively trap volatilized organoselenides for stable selenium isotope analysis. J. Environ. Qual. 40, 1021–1027. https://doi.org/10.2134/jeq2010.0474.

Shraim, A., Chiswell, B., Olszowy, H., 1999. Speciation of arsenic by hydride generation–atomic absorption spectrometry (HG–AAS) in hydrochloric acid reaction medium. Talanta 50, 1109–1127. https://doi.org/10.1016/S0039-9140(99)00221-0.

Skok, A., Manousi, N., Anthemidis, A., Bazel, Y., 2024. Automated systems with fluorescence detection for metal determination: a review. Molecules 29. https://doi.org/10.3390/molecules29235720.

Souza, S.O., Ávila, D.V.L., Cerdà, V., Araujo, R.G.O., 2022. Selenium inorganic speciation in beers using MSFIA-HG-AFS system after multivariate optimization. Food Chem. 367, 130673. https://doi.org/10.1016/j.foodchem.2021.130673.

Suzuki, T., Sturgeon, R.E., Zheng, C., Hioki, A., Nakazato, T., Tao, H., 2012. Influence of speciation on the response from selenium to UV-photochemical vapor generation. Anal. Sci. 28, 807–811. https://doi.org/10.2116/analsci.28.807.

Tarze, A., Dauplais, M., Grigoras, I., Lazard, M., Ha-Duong, N.-T., Barbier, F., Blanquet, S., Plateau, P., 2007. Extracellular production of hydrogen selenide accounts for thiol-assisted toxicity of selenite against saccharomyces cerevisiae. J. Biol. Chem. 282, 8759–8767. https://doi.org/10.1074/jbc.M610078200.

Tian, Y., Xin, F., Jing, J., Zhang, X., 2019. Fluorescence imaging of lysosomal hydrogen selenide under oxygen-controlled conditions. J. Mater. Chem. B 7, 2829–2834. https://doi.org/10.1039/C8TB03169J.

Tutar, B.K., Tutar, Ö.F., Bodur, S., Bakırdere, S., 2025. An analytical approach for inorganic selenium speciation in tap water samples: HPLC – continuous flow hydride generation – FAAS. J. Food Compos. Anal. 147, 108079. https://doi.org/10.1016/j.jfca.2025.108079.

Ueta, I., Kato, D., Nagao, M., 2020. Preconcentration of hydrogen selenide using hydride generation and purge-and-trap collection for the determination of selenium in water samples by atomic absorption spectrometry. Int. J. Environ. Anal. Chem. 17. https://doi.org/10.1080/03067319.2020.1839061.

Wang, N., Tyson, J., 2014. Non-chromatographic speciation of inorganic arsenic by atomic fluorescence spectrometry with flow injection hydride generation with a tetrahydroborate-form anion-exchanger. J. Anal. At. Spectrom. 29, 665–673. https://doi.org/10.1039/C3JA50376C.

Wang, M., Zhong, Y., Qin, J., Zhang, Z., Li, S., Yang, B., 2017. Determination of total selenium in food samples by d-CPE and HG-AFS. Food Chem. 227, 329–334. https://doi.org/10.1016/j.foodchem.2016.11.096.

Wickstrom, T., Lund, W., Bye, R., 1991. Hydride generation atomic absorption spectrometry from alkaline solutions: determination of selenium in copper and nickel materials. J. Anal. At. Spectrom. 6, 389–391. https://doi.org/10.1039/JA9910600389.

Wietecha-Posłuszny, R., Dobrowolska, J., Kościelniak, P., 2006. Method for determination of selenium and arsenic in human urine by atomic fluorescence spectrometry. Anal. Lett. 39, 2787–2796. https://doi.org/10.1080/00032710600867390.

Xin, F., Tian, Y., Zhang, X., 2020. Ratiometric fluorescent probe for highly selective detection of gaseous H2Se. Dyes Pigments 177, 108274. https://doi.org/10.1016/j.dyepig.2020.108274.

Zhou, L., Zheng, W., Sui, Y., Zhu, Z., Li, S., Shi, J., Xiong, T., Cai, F., Wen, J., Zheng, Z., Mei, X., 2025. Characterization of volatile organic compounds in selenium-enriched brown rice tea of different colors using E-nose, HS-GC-IMS and HS-SPME-GC-MS. LWT 224, 117830. https://doi.org/10.1016/j.lwt.2025.117830.

Zou, Z., Deng, Y., Hu, J., Jiang, X., Hou, X., 2018. Recent trends in atomic fluorescence spectrometry towards miniaturized instrumentation-a review. Anal. Chim. Acta 1019, 25–37. https://doi.org/10.1016/j.aca.2018.01.061.